

Analysis of the lepton polarisation asymmetries of $\bar{B} \rightarrow \bar{K}_2(1430) \ell^+ \ell^-$ decay

S. R. Choudhury^{1a}, A. S. Cornell^{2b} and J. D. Roussos^{2c}

¹*Indian Institute of Science Education and Research, Bhopal, India,*

²*National Institute for Theoretical Physics; School of Physics, University of the Witwatersrand, Wits 2050, South Africa*

Abstract

In this work we will study the longitudinal polarisations of both leptons in the decay process $\bar{B} \rightarrow \bar{K}_2(1430) \ell^+ \ell^-$. This process has all the features of the related and well investigated process $\bar{B} \rightarrow \bar{K}^*(890) \ell^+ \ell^-$, with theoretically comparable branching ratios. The polarised differential decay rates as well as the single and double polarisation asymmetries are worked out, where the sensitivity of these to possible right-handed couplings for the related $b \rightarrow s$ radiative decay (and other generic BSM parameters) are also investigated.

1 Introduction

Flavour Changing Neutral Currents (FCNCs) in weak decays provide fertile ground for testing the structure of weak interactions as these decays are forbidden at the tree level. As such, they proceed as higher order loop effects. Consequently they are sensitive to finer details of the basic interactions responsible for the process and therefore provide a natural testing ground for any theories beyond the Standard Model (SM). Of the FCNC decays the radiative mode $B \rightarrow K^*(890) \gamma$ has been experimentally measured, with a lot of theoretical work also having gone into its study. A related decay, $B \rightarrow K_2(1430) \gamma$ [1] has also been observed experimentally, with branching ratios comparable to the decay $B \rightarrow K^*(890) \gamma$. The related decay processes with a lepton pair instead of the photon, which have already been seen for the $K^*(890)$ case, can be expected to be seen for the $K_2(1430)$ case, since the branching ratios are comparable. Analysis of this latter process will therefore be a useful complement to the much investigated analysis for the $K^*(890) \ell^+ \ell^-$ process for confrontation with theory, since the analysis probes the effective Hamiltonian in a similar but not identical way. Data on $K_2(1430) \ell^+ \ell^-$ would thus provide an independent test of the predictions of the SM.

^asrc@iiserbhopal.ac.in

^balan.cornell@wits.ac.za

^cjoe.roussos@gmail.com

In this paper we study the angular distribution of the rare B -decay $\bar{B} \rightarrow \bar{K}_2(1430) \ell^+ \ell^-$ using the standard effective Hamiltonian approach and form factors that have already been estimated for the corresponding radiative decay $\bar{B} \rightarrow \bar{K}_2(1430) \gamma$ [2]. The additional form factors for the dileptonic channel are estimated using the Large Energy Effective Theory (LEET) [3], which enables one to relate the additional form factors to the form factors of the radiative mode. We note here that the LEET does not take account of collinear gluons and this deficiency is remedied in the Soft Collinear Effective theory introduced by Bauer, Fleming, Pirjol and Stewart [4]. However, as they have shown, interactions with collinear gluons preserve the LEET relations between the form factors for a heavy to light decay as long as we ignore terms suppressed by m/E , where m is the mass of the light meson and E is its energy in the B -meson's rest frame.

The importance of polarization effects for the process $B \rightarrow K^* \ell^+ \ell^-$ was first pointed out by Hewett [5] and subsequently by others [6]. These papers considered other observables beyond the differential decay rate. We have earlier considered decay rates [7] for the process under consideration, and in this paper we shall study longitudinal polarization observables in the process. In earlier works τ lepton polarisation asymmetries were analysed in various Beyond the SM (BSM) scenarios for both inclusive and exclusive B decays. Though there is no experimental data on these observables yet, these asymmetries have been observed to be extremely sensitive to the structure of new interactions, making them ideal for testing BSM physics. As such, the paper is organized as follows: In section 2 we will give the relevant effective Hamiltonian and the LEET form factors for the process under consideration. In section 3 we will work out the expressions for the polarised differential decay rate for the semi-leptonic decay mode and the various lepton polarisation asymmetries. We will conclude with our results in section 4.

2 Effective Hamiltonian and Form Factors

The process in which we are interested ($\bar{B} \rightarrow \bar{K}_2(1430) \ell^+ \ell^-$) is governed by the quark level decay $b \rightarrow s \ell^+ \ell^-$. By integrating out the heavy degrees of freedom from the theory we obtain the effective Hamiltonian [8]:

$$\begin{aligned} \mathcal{H}^{eff} = \frac{\alpha G_F}{\sqrt{2}\pi} V_{tb} V_{ts}^* \left[-iC_{7L} m_b \frac{q^\nu}{q^2} (T_{\mu\nu} + T_{\mu\nu}^5) L^\mu - iC_{7R} m_b \frac{q^\nu}{q^2} (T_{\mu\nu} - T_{\mu\nu}^5) L^\mu \right. \\ \left. + \frac{1}{2} (C_9^{eff} - C_{10}) (V - A)_\mu (L^\mu - L_5^\mu) \right. \\ \left. + \frac{1}{2} (C_9^{eff} + C_{10}) (V - A)_\mu (L^\mu + L_5^\mu) \right]. \end{aligned} \quad (1)$$

where $L^\mu = \bar{\ell} \gamma^\mu \ell$ and $L_5^\mu = \bar{\ell} \gamma^\mu \gamma_5 \ell$ are the lepton bilinears, whilst the C 's are the Wilson coefficients. C_{7R} in the SM is zero but may arise in models BSM. As such we will retain this in order to see its effect on some of the experimentally observable quantities. C_9^{eff} includes the short-distance Wilson coefficient as well as long distance effects simulated through the lepton

pair being produced by decay of $c\bar{c}$ resonances, where these are fully spelled out in appendix B. Note also that in equation (1) we have used the $(V - A)$ structure for the hadronic part (except for C_7)

$$V_\mu = (\bar{s}\gamma_\mu b) \quad , \quad (2)$$

$$A_\mu = (\bar{s}\gamma_\mu\gamma_5 b) \quad , \quad (3)$$

$$T_{\mu\nu} = (\bar{s}\sigma_{\mu\nu} b) \quad , \quad (4)$$

$$T_{\mu\nu}^5 = (\bar{s}\sigma_{\mu\nu}\gamma_5 b) \quad . \quad (5)$$

Note that this structure doesn't change under the transformation $V \leftrightarrow -A$ and $T_{\mu\nu} \leftrightarrow T_{\mu\nu}^5$. Furthermore, we can relate the hadronic factors of $T_{\mu\nu}$ and $T_{\mu\nu}^5$ by using the identity¹:

$$\sigma_{\mu\nu} = -\frac{i}{2}\varepsilon^{\mu\nu\rho\delta}\sigma_{\rho\delta}\gamma_5 \quad .$$

In order to enable us to study the sensitivity of our results to BSM physics, we have included a possible C_{7R} in the effective Hamiltonian, which is otherwise absent in the SM. This is similar to the work of Kim *et al.*[9] for the decay channel $B \rightarrow K^*(890)\ell^+\ell^-$. Physics BSM often results in non-standard Z' coupling to quarks. As far as the effective Hamiltonian is concerned, this results in modifying the values of C_9 and C_{10} away from their SM values. Following, a recent study of such deviations and the constraints imposed on them from known experimental data [10], we write additive complements to both C_9 and C_{10} that we will detail later.

We now define the hadronic form factors for the $\bar{B} \rightarrow \bar{K}_2(1430)$ decay as:

$$\langle K_2(p')|V_\mu|B(p)\rangle = 2V\epsilon^{*\alpha\beta}\varepsilon_{\alpha\mu\nu\rho}p^\nu p^\rho p_\beta \quad , \quad (6)$$

$$\langle K_2(p')|A_\mu|B(p)\rangle = \epsilon^{*\alpha\beta}\left[2A_1g_{\alpha\mu}p_\beta + A_2p_\alpha p_\beta p_\mu + A_3p_\alpha p_\beta p'_\mu\right] \quad , \quad (7)$$

$$\langle K_2(p')|iT_{\mu\nu}q^\nu|B(p)\rangle = \frac{2iU_1}{m_B}\epsilon^{*\alpha\beta}\varepsilon_{\mu\alpha\lambda\rho}p_\beta p^\lambda p'^\rho \quad , \quad (8)$$

$$\begin{aligned} \langle K_2(p')|iT_{\mu\nu}^5q^\nu|B(p)\rangle &= \epsilon^{*\alpha\beta}\left(\frac{U_2(p+p')_\beta}{m_B}\right)\left[g_{\mu\alpha}(p+p')\cdot q - (p+p')_\mu q^\alpha\right] \\ &\quad -\epsilon^{*\alpha\beta}p_\alpha p_\beta\left[q_\mu - (p+p')_\mu\frac{q^2}{(p+p')\cdot q}\right]\frac{U_3}{m_B} \quad , \end{aligned} \quad (9)$$

where $\epsilon^{*\alpha\beta}$ is the polarisation vector for the K_2 .

This leads to a matrix element:

$$\mathcal{M} = \left(\frac{\alpha G_F \lambda_{CKM}}{2\sqrt{2}\pi}\right)\epsilon^{*\alpha\beta}\left[(L^\mu)H_{\mu\alpha\beta}^V + (L_5^\mu)H_{\mu\alpha\beta}^A\right] \quad , \quad (10)$$

¹Where we have used the convention that $\gamma_5 = i\gamma^0\gamma^1\gamma^2\gamma^3$ and that $\varepsilon_{0123} = 1$.

where

$$H_{\mu\alpha\beta}^A = C_{10} \left[2V \varepsilon_{\alpha\mu\nu\rho} p^\nu p^\rho p_\beta - 2A_1 g_{\alpha\mu} p_\beta - A_2 p_\alpha p_\beta p_\mu - A_3 p_\alpha p_\beta p'_\mu \right], \quad (11)$$

$$\begin{aligned} H_{\mu\alpha\beta}^V = C_9^{eff} & \left[2V \varepsilon_{\alpha\mu\nu\rho} p^\nu p^\rho p_\beta - 2A_1 g_{\alpha\mu} p_\beta - A_2 p_\alpha p_\beta p_\mu - A_3 p_\alpha p_\beta p'_\mu \right] \\ & - 2(C_{7L} + C_{7R}) \frac{m_b}{q^2} \times \left(\frac{2iU_1}{m_B} \varepsilon_{\mu\alpha\lambda\rho} p_\beta p^\lambda p'^\rho \right) \\ & + 2(C_{7L} - C_{7R}) \frac{m_b}{q^2} \times \left(\frac{U_2(p+p')_\beta}{m_B} \right) \left[g_{\mu\alpha}(p+p') \cdot q - (p+p')_\mu q^\alpha \right] \\ & + 2(C_{7L} - C_{7R}) \frac{m_b}{q^2} \times \left(p_\alpha p_\beta \left[q_\mu - (p+p')_\mu \frac{q^2}{(p+p') \cdot q} \right] \frac{U_3}{m_B} \right). \end{aligned} \quad (12)$$

The helicity states for the K_2 are:

$$\begin{aligned} \epsilon^{*\alpha\beta}(+2) &= \epsilon_{(+)}^\alpha \epsilon_{(+)}^\beta \\ \epsilon^{*\alpha\beta}(+1) &= \frac{1}{\sqrt{2}} \left(\epsilon_{(+)}^\alpha \epsilon_{(0)}^\beta + \epsilon_{(0)}^\alpha \epsilon_{(+)}^\beta \right) \\ \epsilon^{*\alpha\beta}(+2) &= \frac{1}{\sqrt{6}} \left(\epsilon_{(+)}^\alpha \epsilon_{(-)}^\beta + \epsilon_{(-)}^\alpha \epsilon_{(+)}^\beta \right) + \sqrt{\frac{2}{3}} \epsilon_{(0)}^\alpha \epsilon_{(0)}^\beta \\ \epsilon^{*\alpha\beta}(-1) &= \frac{1}{\sqrt{2}} \left(\epsilon_{(-)}^\alpha \epsilon_{(0)}^\beta + \epsilon_{(0)}^\alpha \epsilon_{(-)}^\beta \right) \\ \epsilon^{*\alpha\beta}(-2) &= \epsilon_{(-)}^\alpha \epsilon_{(-)}^\beta, \end{aligned} \quad (13)$$

where

$$\begin{aligned} [\epsilon_{(+)}^\mu] &= \frac{1}{\sqrt{2}} (0, -i, \cos \theta, -\sin \theta) \\ [\epsilon_{(0)}^\mu] &= \frac{1}{m_K} (k, 0, E_K \sin \theta, E_K \cos \theta) \\ [\epsilon_{(-)}^\mu] &= \frac{1}{\sqrt{2}} (0, -i, -\cos \theta, \sin \theta), \end{aligned} \quad (14)$$

and the lepton bilinears L^μ and L_5^μ are given by (for lepton helicity (λ_1, λ_2)):

$$\begin{aligned}
[L^\mu(+, +)] &= (0, 0, 0, 1) \\
[L^\mu(+, -)] &= (0, E_\ell/m_\ell, iE_\ell/m_\ell, 0) \\
[L^\mu(-, +)] &= (0, E_\ell/m_\ell, -iE_\ell/m_\ell, 0) \\
[L^\mu(-, -)] &= (0, 0, 0, -1) \\
[L_5^\mu(+, +)] &= (1, 0, 0, 0) \\
[L_5^\mu(+, -)] &= (0, -p_\ell/m_\ell, -ip_\ell/m_\ell, 0) \\
[L_5^\mu(-, +)] &= (0, p_\ell/m_\ell, -ip_\ell/m_\ell, 0) \\
[L_5^\mu(-, -)] &= (1, 0, 0, 0) .
\end{aligned} \tag{15}$$

The form factors introduced in equations (6–9) can be related using the LEET approach, that is, using equations (44–48) of J. Charles *et al.* [3] we get:

$$\begin{aligned}
V &= \frac{iA_1}{m_B E} , \\
V &= -\frac{iU_1}{m_B^2} , \\
U_2 &= -2A_1 , \\
A_2 &= 0 , \\
A_3 &= \frac{2U_3}{m_B^2} ,
\end{aligned} \tag{16}$$

where we have taken the limit of the heavy quark mass going to infinity and $E = p \cdot p' / m_B$. Note that with this approach we have introduced no extra hadronic form factors beyond what is required for the radiative mode. Thus, once we are able to describe the radiative mode we have in effect a check on the model from the dileptonic mode. The radiative mode form factors U_1 , U_2 and U_3 have been given by Cheng and Chua [2] in their analysis of radiative charmless decays of the B -meson using covariant light cone wave functions. We shall use their results.

3 Kinematics and the lepton polarisation asymmetries

If we now use the dilepton centre of mass (CM) frame, where θ shall be the angle between the K_2 meson and the ℓ^+ , and s is the energy squared of the outgoing leptons, then we can write our polarised differential decay widths as:

$$\frac{d\Gamma_{ij}^k}{dsd(\cos\theta)} = (2m_\ell)^2 \frac{\alpha^2 G_F^2}{2^{12} \pi^5 m_B^3} |V_{tb} V_{ts}^*|^2 \sqrt{1 - \frac{4m_\ell^2}{s}} \lambda^{1/2} |\mathcal{M}_{ij}^k|^2 , \tag{17}$$

where we have written our amplitudes as \mathcal{M}_{ij}^k with i as the ℓ^+ helicity, j as the ℓ^- helicity and k the K_2 's helicity, where all $k = \pm 2$ were found to be zero:

$$\begin{aligned}
\mathcal{M}_{++}^\pm &= \sin \theta (C_{7L}(\mp H_2 - H_1) + C_{7R}(\mp H_2 - H_1) \mp C_9(H_3 \pm H_4)) , \\
\mathcal{M}_{+-}^\pm &= \frac{1}{2} (1 \mp \cos \theta) \left(\frac{i\sqrt{s}}{m_\ell} \right) \left(C_{7L}(\mp H_1 + H_2) + C_{7R}(-H_2 \mp H_1) \right. \\
&\quad \left. + \sqrt{1 - \frac{4m_\ell^2}{s}} C_{10}(H_3 \pm H_4) - C_9(H_3 \pm H_4) \right) , \\
\mathcal{M}_{-+}^\pm &= \frac{1}{2} (1 \pm \cos \theta) \left(\frac{i\sqrt{s}}{m_\ell} \right) \left(C_{7L}(-H_1 + H_2) + C_{7R}(-H_2 - H_1) \right. \\
&\quad \left. + \sqrt{1 - \frac{4m_\ell^2}{s}} C_{10}(-H_3 \mp H_4) - C_9(H_3 + H_4) \right) , \\
\mathcal{M}_{--}^\pm &= \sin \theta (C_{7L}(\mp H_2 - H_1) + C_{7R}(\pm H_2 - H_1) + C_9(\pm H_3 - H_4)) , \\
\mathcal{M}_{\pm\pm}^0 &= \cos \theta (\pm(C_{7L} - C_{7R})(Z_1 + Z_2) \pm C_9 Y_2) + Y_1 C_{10} , \\
\mathcal{M}_{\pm\mp}^0 &= \sin \theta \left(\frac{i\sqrt{s}}{m_\ell} \right) \left(\pm Y_2 C_9 \pm (C_{7L} - C_{7R})(Z_1 + Z_2) - \sqrt{1 - \frac{4m_\ell^2}{s}} C_{10} Y_2 \right) , \tag{18}
\end{aligned}$$

where

$$\begin{aligned}
H_1 &= \frac{m_b \lambda U_1}{2m_B m_K s} \\
H_2 &= \frac{m_b \lambda^{1/2} (m_B^2 - m_K^2) U_2}{2m_B m_K s} \\
H_3 &= \frac{2\lambda^{1/2} A_1}{4m_K} \\
H_4 &= \frac{iV\lambda}{4m_K} \\
Z_1 &= \frac{m_b \lambda^{1/2}}{\sqrt{6} m_K^2 m_B s^{3/2}} U_2 (\lambda - (m_B^2 - m_K^2)(m_B^2 - m_K^2 - s)) \\
Z_2 &= \frac{m_b \lambda^{3/2} U_3}{\sqrt{6} (m_B^3 m_K^2 - m_B m_K^4) \sqrt{s}} \\
Y_1 &= \frac{\lambda}{4\sqrt{6} m_K^2 \sqrt{s}} (-4A_1 - (m_B^2 - m_K^2)(A_2 + A_3) + (A_3 - A_2)s) \\
Y_2 &= \frac{\lambda^{1/2}}{4\sqrt{6} m_K^2 \sqrt{s}} ((A_2 + A_3)\lambda + 4A_1(m_B^2 - m_K^2 - s)) \\
\text{and } \lambda &= m_B^4 + m_K^4 + s^2 - 2m_B^2 m_K^2 - 2sm_B^2 - 2sm_K^2 . \tag{19}
\end{aligned}$$

Equipped with the above we can now define the various single lepton and double lepton polarisation asymmetries. The single lepton longitudinal polarisation asymmetries are defined

as:

$$\begin{aligned}
\mathcal{P}_{\ell^+\ell^+}^\pm &= \left[\pm \left(\frac{d\Gamma_{++}^+}{ds} + \frac{d\Gamma_{-+}^+}{ds} + \frac{d\Gamma_{++}^0}{ds} + \frac{d\Gamma_{-+}^0}{ds} + \frac{d\Gamma_{++}^-}{ds} + \frac{d\Gamma_{-+}^-}{ds} \right) \right. \\
&\quad \left. \mp \left(\frac{d\Gamma_{+-}^+}{ds} + \frac{d\Gamma_{--}^+}{ds} + \frac{d\Gamma_{+-}^0}{ds} + \frac{d\Gamma_{--}^0}{ds} + \frac{d\Gamma_{+-}^-}{ds} + \frac{d\Gamma_{--}^-}{ds} \right) \right] \Big/ \frac{d\Gamma_{tot}}{ds}, \\
\mathcal{P}_{\ell^+\ell^-}^\pm &= \left[\pm \left(\frac{d\Gamma_{++}^+}{ds} + \frac{d\Gamma_{+-}^+}{ds} + \frac{d\Gamma_{++}^0}{ds} + \frac{d\Gamma_{+-}^0}{ds} + \frac{d\Gamma_{++}^-}{ds} + \frac{d\Gamma_{+-}^-}{ds} \right) \right. \\
&\quad \left. \mp \left(\frac{d\Gamma_{-+}^+}{ds} + \frac{d\Gamma_{--}^+}{ds} + \frac{d\Gamma_{-+}^0}{ds} + \frac{d\Gamma_{--}^0}{ds} + \frac{d\Gamma_{-+}^-}{ds} + \frac{d\Gamma_{--}^-}{ds} \right) \right] \Big/ \frac{d\Gamma_{tot}}{ds}. \quad (20)
\end{aligned}$$

Along the same lines we can also define the double lepton polarisation asymmetries:

$$\begin{aligned}
\mathcal{P}_{\ell^+\ell^-}^{\pm\pm} &= \left\{ \left[\left(\frac{d\Gamma_{++}^+}{ds} + \frac{d\Gamma_{++}^0}{ds} + \frac{d\Gamma_{++}^-}{ds} \right) \mp \left(\frac{d\Gamma_{+-}^+}{ds} + \frac{d\Gamma_{+-}^0}{ds} + \frac{d\Gamma_{+-}^-}{ds} \right) \right] \right. \\
&\quad \left. \mp \left[\left(\frac{d\Gamma_{-+}^+}{ds} + \frac{d\Gamma_{-+}^0}{ds} + \frac{d\Gamma_{-+}^-}{ds} \right) \mp \left(\frac{d\Gamma_{--}^+}{ds} + \frac{d\Gamma_{--}^0}{ds} + \frac{d\Gamma_{--}^-}{ds} \right) \right] \right\} \Big/ \frac{d\Gamma_{tot}}{ds}, \\
\mathcal{P}_{\ell^+\ell^-}^{\pm\mp} &= \left\{ \left[\left(\frac{d\Gamma_{++}^+}{ds} + \frac{d\Gamma_{++}^0}{ds} + \frac{d\Gamma_{++}^-}{ds} \right) \mp \left(\frac{d\Gamma_{+-}^+}{ds} + \frac{d\Gamma_{+-}^0}{ds} + \frac{d\Gamma_{+-}^-}{ds} \right) \right] \right. \\
&\quad \left. \pm \left[\left(\frac{d\Gamma_{-+}^+}{ds} + \frac{d\Gamma_{-+}^0}{ds} + \frac{d\Gamma_{-+}^-}{ds} \right) \mp \left(\frac{d\Gamma_{--}^+}{ds} + \frac{d\Gamma_{--}^0}{ds} + \frac{d\Gamma_{--}^-}{ds} \right) \right] \right\} \Big/ \frac{d\Gamma_{tot}}{ds}. \quad (21)
\end{aligned}$$

Note that in these asymmetries we have divided by the total differential decay width

$$\frac{d\Gamma_{tot}}{ds} = \sum_{ijk} \frac{d\Gamma_{ij}^k}{ds}.$$

4 Results and Conclusion

We have followed reference [9] for the form of the parameterisation of C_{7L} and C_{7R} , which automatically takes care of the constraints imposed by experimental data on the radiative decay. Also, it can take into account the possibility that the phase of this term from the SM value ($u = v = 0$), although present in the pure radiative decay, would not show up:

$$\begin{aligned}
C_{7L} &= -\sqrt{0.081} \cos x \exp(i(u+v)) \quad , \\
C_{7R} &= -\sqrt{0.081} \sin x \exp(i(u-v)) \quad . \quad (22)
\end{aligned}$$

To also take into account possible BSM effects on the other SM Wilson coefficients, we write [10]:

$$C_9 = C_9^{SM} + z \quad , \quad (23)$$

$$C_{10} = -4.546 + y \quad , \quad (24)$$

(x, u, v)	$(0, 0, 0)$	$(\pi/4, 0, 0)$	$(-\pi/4, 0, 0)$	$(\arctan(0.5), 0, 0)$	$(\pi/2, 0, 0)$
C_{7R}/C_{7L}	0	- 1	+ 1	0.5	$C_{7L}/C_{7R} = 0$
$s(\text{for } \mathcal{P}_{\mu^+}^+ = 0) \text{ (GeV}^2\text{)}$					
$y = z = 0$	–	1.7891	0.2925	–	0.5448
$y = 5, z = -10$	–	–	0.1779	–	2.2844
$y = 5, z = 7.5$	2.1747	1.9146	2.3095	2.3330	1.5243
$y = 10, z = -5$	8.0627	8.5000	–	6.7992	–
$s(\text{for } \mathcal{P}_{\mu^-}^+ = 0) \text{ (GeV}^2\text{)}$					
$y = z = 0$	–	1.7911	–	–	0.5449
$y = 5, z = -10$	–	0.1869	–	–	2.2844
$y = 5, z = 7.5$	2.0739	1.8835	2.2496	2.2507	1.5243
$y = 10, z = -5$	8.0638	8.5003	1.5142	6.8028	–

Table 1: Zeroes of the muon polarisation asymmetries for $s > 4m_\mu^2$ and below $s \lesssim 9.6(\text{GeV})^2$. Several values of the BSM parameters x, y, z are presented (where we consider only $u = v = 0$).

where C_9^{SM} is defined in appendix B. z and y above are constrained from radiative and dileptonic decay data by [10]:

$$\begin{aligned}
z &< -4.344 \text{ ,} \\
y &> +4.669 \text{ ,} \\
1.05(z + 4.01)^2 + 1.05(y + 4.669)^2 &< 59.58 \text{ ,} \\
0.61(z + 3.89)^2 + 0.61(y + 4.669)^2 &> 6.38 \text{ .}
\end{aligned} \tag{25}$$

This way of parametrizing possible deviations from SM values takes into account the following facts: The decay rates for radiative and dileptonic $K^*(890)$ decay modes of B -mesons are in reasonable agreement with SM values. However, the most significant deviation from SM predictions seems to be in the recent data of the FB asymmetry for the decay $B \rightarrow K^*(890) \ell^+ \ell^-$ [11]. Within the context of the effective Hamiltonian, equation (1), such deviations can be accommodated, without significantly disturbing the predictions for the decay rates, by changing the relative signs of the Wilson co-efficients C_9 and C_{10} relative to C_7 . The parametrization above does just that.

With this parameterisation we calculate the various lepton polarisation asymmetries and plot in figures 1 to 3 for some typical values of (x, u, v) , and give the zeroes of these plots in table 1². The results show sensitivity to the values of x, y and z quite clearly, where data on the dileptonic decay mode of the $\bar{B} \rightarrow \bar{K}_2(1430) \ell^+ \ell^-$ would be very useful in testing physics BSM. Note that we have restricted our attention to the large recoil region, where we expect the LEET to be more valid. The zeroes of the various lepton polarisation asymmetries, which is a

²For $\mathcal{P}_{\mu^-}^+(y = 5, z = 7.5) = 0$ we only present the zeroes near $s = 2(\text{GeV})^2$

crucial index for comparison with experimental data [12], fortunately falls well within this region for most choices of the BSM parameters. We expect that experimental measurements of this dileptonic mode will be available in the near future and the comparison of those with the present theoretical estimates would provide a very useful complement to the corresponding analysis of the well established $K^*(890)$ case.

Furthermore, a paper recently appeared from the Belle collaboration [11] and has given indications of new physics BSM, which could be of the type suggested by our equation (22) with non-zero phases. Therefore, it would be interesting to also experimentally measure the lepton polarisation asymmetries in $\bar{B} \rightarrow \bar{K}_2(1430)$ transitions, such as we are proposing. For the decay of $B \rightarrow K^*(890) \ell^+ \ell^-$, the Belle result had only 230 events. The number of events into the corresponding $K_2(1430)$ may be expected to be about half this number making the statistics even more limited. However, the statistics would drastically improve when data from LHCb becomes available. Estimates made in reference [14] for the LHCb collaboration show that the $B \rightarrow K^*(890) \ell^+ \ell^-$ would have about 8000 events annually, making the analysis of the FB asymmetry more definitive. The corresponding decay channel $B \rightarrow K_2(1430) \ell^+ \ell^-$ considered here would also have a few thousand events making for meaningful comparisons with the SM and theories beyond possible.

Acknowledgements

SRC would like to acknowledge the Department of Science and Technology, Government of India, for support through a research project.

A The form factors

We shall take the form factors U_1 , U_2 and U_3 from Cheng *et al.* [2]; the remaining form factors can be related to these using the relations in Charles *et al.* [3] as spelt out earlier:

$$\begin{aligned}
 U_1(s) &= \frac{0.19}{1 - 2.22(s/m_B^2) + 2.13(s/m_B^2)^2} \ , \\
 U_2(s) &= \frac{0.19}{(1 - s/m_B^2)(1 - 1.77(s/m_B^2) + 4.32(s/m_B^2)^2)} \ , \\
 U_3(s) &= \frac{0.16}{1 - 2.19(s/m_B^2) + 1.80(s/m_B^2)^2} \ .
 \end{aligned}$$

B Input parameters and Wilson coefficients

The input parameters used in the generation of the numerical results are as follows:

$$m_B = 5.26\text{GeV} \quad , \quad m_{K^*} = 1.43\text{GeV} \quad , \quad m_b = 4.8\text{GeV} \quad , \quad m_c = 1.4\text{GeV} \ ,$$

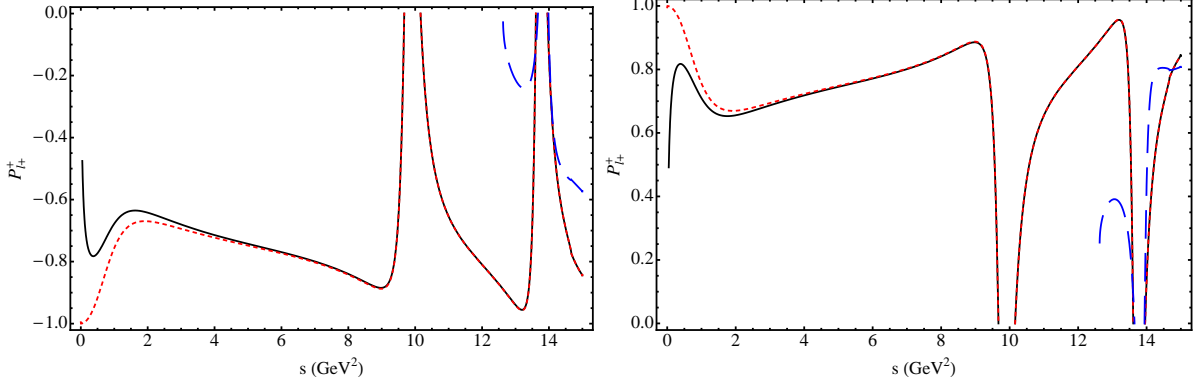


Figure 1: (Colour online) The single lepton polarisation asymmetries ($\mathcal{P}_{\ell^+}^\lambda$) for a range of values for the three lepton species: (Black) solid line for muons, (Red) dotted line for electrons, and (Blue) dashed line for taus. The left panel is for $\lambda = +$, the right panel $\lambda = -$, these are for $x = u = v = y = z = 0$.

$$\begin{aligned}
m_s &= 0.1\text{GeV} \quad , \quad \mathcal{B}(J/\psi(1S) \rightarrow \ell^+\ell^-) = 6 \times 10^{-2} \quad , \\
m_{J/\psi(1S)} &= 3.097\text{GeV} \quad , \quad \mathcal{B}(\psi(2S) \rightarrow \ell^+\ell^-) = 8.3 \times 10^{-3} \quad , \\
m_{\psi(2S)} &= 3.097\text{GeV} \quad , \quad \Gamma_{\psi(2S)} = 0.277 \times 10^{-3}\text{GeV} \quad , \\
\Gamma_{J/\psi(1S)} &= 0.088 \times 10^{-3}\text{GeV} \quad , \quad V_{tb}V_{ts}^* = 0.0385 \quad , \quad \alpha = \frac{1}{129} \quad , \quad G_F = 1.17 \times 10^{-5} \text{GeV}^{-2}.
\end{aligned}$$

The Wilson coefficients used were as in Kim *et al.* [9], namely:

$$\begin{aligned}
C_{7L} &= -\sqrt{0.081} \cos x \exp(i(u+v)) \quad , \\
C_{7R} &= -\sqrt{0.081} \sin x \exp(i(u-v)) \quad , \\
C_{10} &= -4.546 \quad ,
\end{aligned}$$

$$\begin{aligned}
C_9^{SM} &= 4.153 + 0.381g\left(\frac{m_c}{m_b}, \frac{s}{m_B^2}\right) + 0.033g\left(1, \frac{s}{m_B^2}\right) + 0.032g\left(0, \frac{s}{m_B^2}\right) - 0.381 \times 2.3 \times \frac{3\pi}{\alpha} \\
&\times \left(\frac{\Gamma_{\psi(2S)} \mathcal{B}(\psi(2S) \rightarrow \ell^+\ell^-) m_{\psi(2S)}}{s - m_{\psi(2S)}^2 + im_{\psi(2S)} \Gamma_{\psi(2S)}} + \frac{\Gamma_{J/\psi(1S)} \mathcal{B}(J/\psi(1S) \rightarrow \ell^+\ell^-) m_{J/\psi(1S)}}{s - m_{J/\psi(1S)}^2 + im_{J/\psi(1S)} \Gamma_{J/\psi(1S)}} \right) ,
\end{aligned}$$

where the function g is taken from reference [15]:

$$\begin{aligned}
g(\hat{m}_i, \hat{s}) &= -\frac{8}{9} \ln(\hat{m}_i) + \frac{8}{27} + \frac{4}{9} \left(\frac{4\hat{m}_i^2}{\hat{s}} \right) - \frac{2}{9} \left(2 + \frac{4\hat{m}_i^2}{\hat{s}} \right) \sqrt{\left| 1 - \frac{4\hat{m}_i^2}{\hat{s}} \right|} \\
&\times \begin{cases} \left| \ln \left(\frac{1 + \sqrt{1 - 4\hat{m}_i^2/\hat{s}}}{1 - \sqrt{1 - 4\hat{m}_i^2/\hat{s}}} \right) - i\pi \right| , & 4\hat{m}_i^2 < \hat{s} \\ 2 \arctan \frac{1}{\sqrt{4\hat{m}_i^2/\hat{s} - 1}} , & 4\hat{m}_i^2 > \hat{s} \end{cases} .
\end{aligned}$$

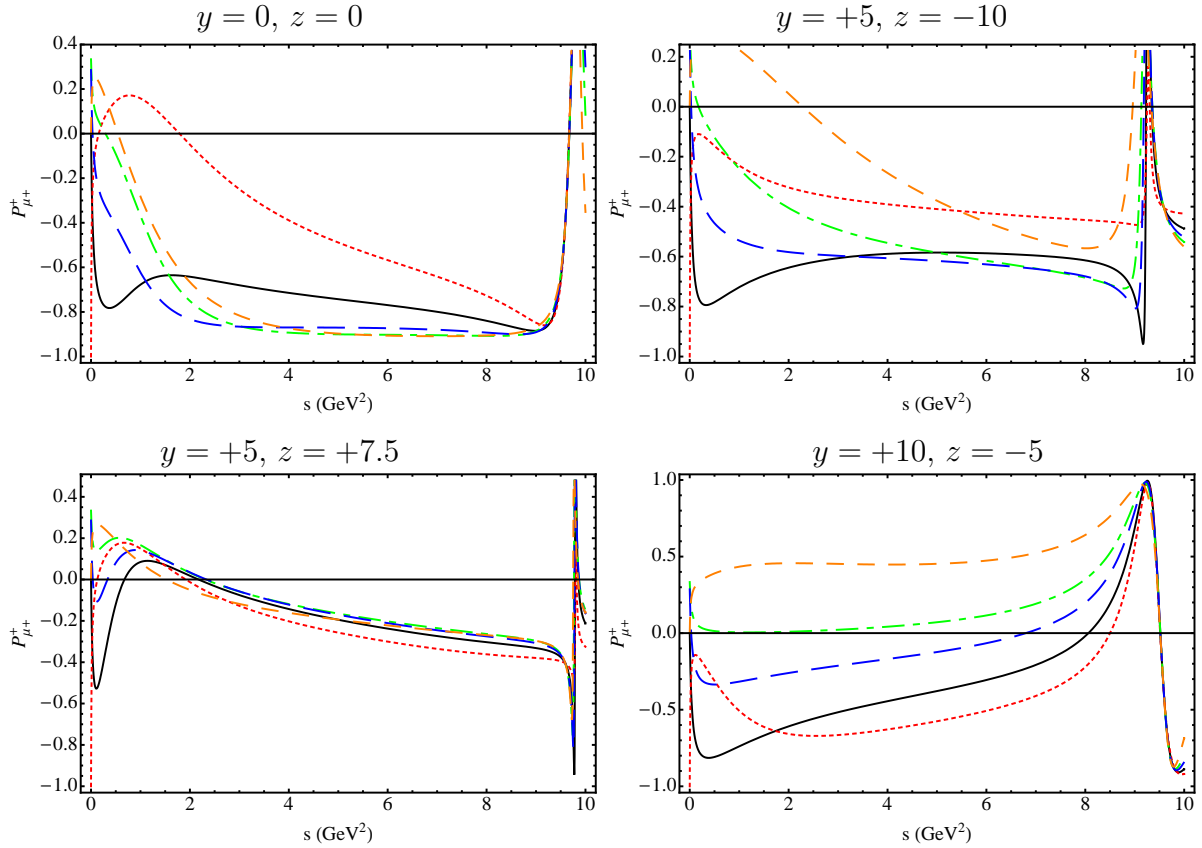


Figure 2: (Colour online) The normalised single muon polarisation asymmetry ($\mathcal{P}_{\mu^+}^+$) for a range of values for C_{7L} and C_{7R} : $C_{7L}/C_{7R} = 0$ (Black) solid line, $C_{7L}/C_{7R} = +1$ (Red) dotted line, $C_{7L}/C_{7R} = -1$ (Green) dot-dashed line, $C_{7L}/C_{7R} = 0.5$ (Blue) dashed line, and $C_{7R}/C_{7L} = 0$ (Orange) small dashed line. The top left panel is for $y = 0, z = 0$, the top right panel for $y = +5, z = -10$, whilst the bottom left panel is for $y = +5, z = -7.5$ and the bottom right panel is for $y = +10$ and $z = -5$.

References

- [1] B. Aubert *et al.* [BABAR Collaboration], Phys. Rev. D **70**, 091105 (2004) [arXiv:hep-ex/0409035]; S. Nishida *et al.* [Belle Collaboration], Phys. Rev. Lett. **89**, 231801 (2002) [arXiv:hep-ex/0205025].
- [2] H. Y. Cheng and C. K. Chua, Phys. Rev. D **69**, 094007 (2004) [arXiv:hep-ph/0401141].
- [3] M. J. Dugan and B. Grinstein, Phys. Lett. B **255**, 583 (1991); J. Charles, A. Le Yaouanc, L. Oliver, O. Pene and J. C. Raynal, Phys. Rev. D **60**, 014001 (1999) [arXiv:hep-ph/9812358].
- [4] C. W. Bauer, S. Fleming, D. Pirjol and I. W. Stewart, Phys. Rev. D **63**, 114020 (2001) [arXiv:hep-ph/0011336].
- [5] J. L. Hewett, Phys. Rev. **D53**, 4964-4969 (1996). [hep-ph/9506289].

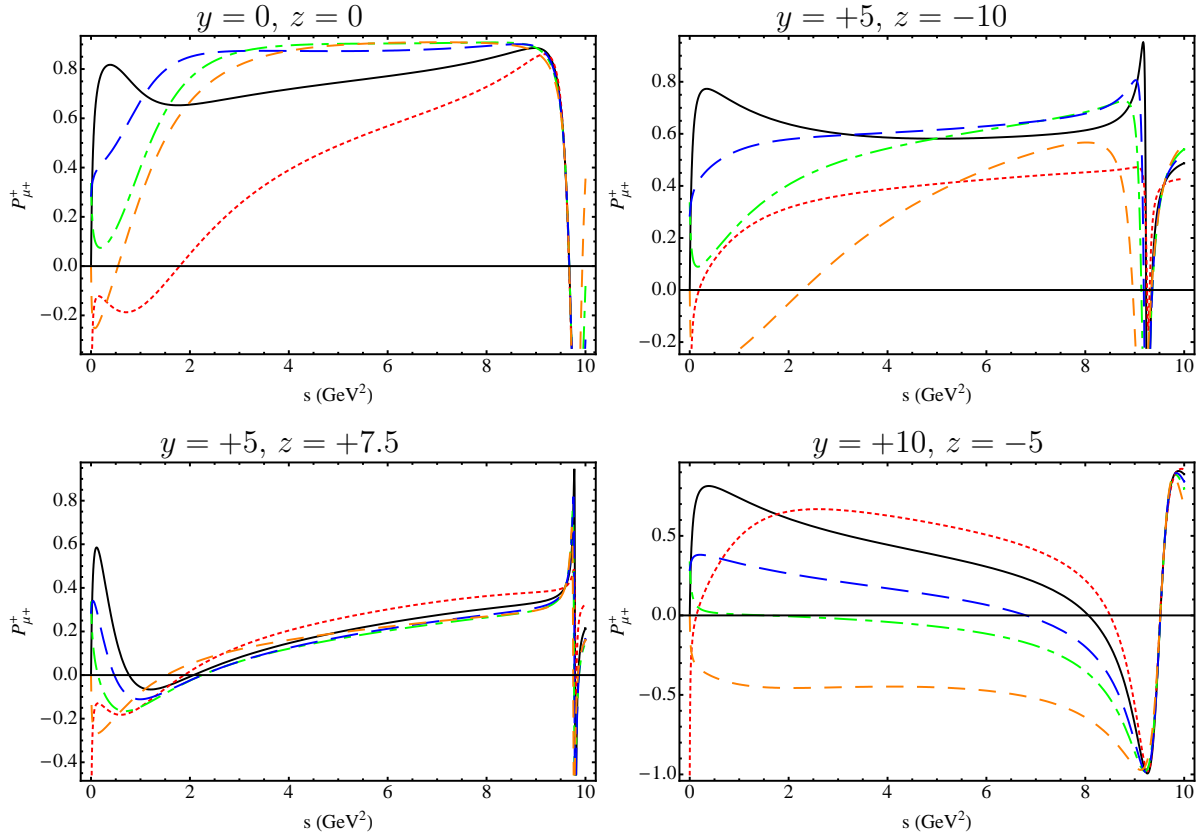


Figure 3: (Colour online) The normalised single muon polarisation asymmetry ($\mathcal{P}_{\mu^+}^+$) for a range of values for C_{7L} and C_{7R} : $C_{7L}/C_{7R} = 0$ (Black) solid line, $C_{7L}/C_{7R} = +1$ (Red) dotted line, $C_{7L}/C_{7R} = -1$ (Green) dot-dashed line, $C_{7L}/C_{7R} = 0.5$ (Blue) dashed line, and $C_{7R}/C_{7L} = 0$ (Orange) small dashed line. The top left panel is for $y = 0, z = 0$, the top right panel for $y = +5, z = -10$, whilst the bottom left panel is for $y = +5, z = -7.5$ and the bottom right panel is for $y = +10$ and $z = -5$.

- [6] F. Kruger, L. M. Sehgal, Phys. Lett. **B380**, 199-204 (1996). [hep-ph/9603237]; S. R. Choudhury, N. Gaur, Phys. Rev. **D66**, 094015 (2002). [hep-ph/0206128]; T. M. Aliev, M. K. Cakmak, M. Savci, Nucl. Phys. **B607**, 305-325 (2001). [hep-ph/0009133]; G. Erkol, G. Turan, JHEP **0202**, 015 (2002). [hep-ph/0201055].
- [7] S. R. Choudhury, A. S. Cornell and N. Gaur, Phys. Rev. D **81**, 094018 (2010) [arXiv:0911.4783 [hep-ph]].
- [8] For a review with complete references, see: A. Ali, Int. J. Mod. Phys. A **20**, 5080 (2005) [arXiv:hep-ph/0412128]; G. Buchalla, A. J. Buras and M. E. Lautenbacher, Rev. Mod. Phys. **68**, 1125 (1996) [arXiv:hep-ph/9512380].
- [9] C. S. Kim, Y. G. Kim, C. D. Lu and T. Morozumi, Phys. Rev. D **62**, 034013 (2000) [arXiv:hep-ph/0001151].

- [10] C. W. Chiang, R. H. Li and C. D. Lu, arXiv:0911.2399 [hep-ph].
- [11] J. T. Wei *et al.* [BELLE Collaboration], Phys. Rev. Lett. **103**, 171801 (2009) [arXiv:0904.0770 [hep-ex]].
- [12] A. Ali, P. Ball, L. T. Handoko and G. Hiller, Phys. Rev. D **61**, 074024 (2000) [arXiv:hep-ph/9910221].
- [13] H. Hatanaka and K. C. Yang, Phys. Rev. D **79**, 114008 (2009) [arXiv:0903.1917 [hep-ph]].
- [14] See for example H. Ruiz [LHCb Collaboration], J. Phys. Conf. Ser. **171**, 012057 (2009).
- [15] M. Misiak, Nucl. Phys. B **393**, 23 (1993) [Erratum-ibid. B **439**, 461 (1995)]. A. J. Buras and M. Munz, Phys. Rev. D **52**, 186 (1995) [arXiv:hep-ph/9501281].
- [16] P. Colangelo, F. De Fazio, R. Ferrandes and T. N. Pham, Phys. Rev. D **73**, 115006 (2006) [arXiv:hep-ph/0604029].